The effect of surface diffusibility on the collective modes of metal clusters

1999 J. Phys.: Condens. Matter 11 8459

(http://iopscience.iop.org/0953-8984/11/43/309)

J. Phys.: Condens. Matter **11** (1999) 8459–8476. Printed in the UK PII: S0953-8984(99)04450-1

The effect of surface diffusibility on the collective modes of metal clusters

João da Providência Jr† and Maria Begoña Torres‡

† Departamento de Física, Universidade de Coimbra, P-3000 Coimbra, Portugal
‡ Departamento de Matemáticas y Computación, Universidad de Burgos, E-09006 Burgos, Spain

Received 21 May 1999

Abstract. We calculate the eigenmode spectrum for collective multipole vibrations of the electrons of alkali clusters including coupling between surface and volume plasmons. We formulate the equations of motion for the collective variables (density and velocity potential) starting from the hydrodynamic approximation. We investigate the effect of the diffusibility of the valence electrons on their collective modes, considering an equilibrium density of the valence electrons with a smooth surface profile. This effect was not considered in previous work carried out by the first author, who assumed the equilibrium density of the valence electrons to be a constant that has the bulk value. The results indicate that, within the hydrodynamic model, surface spill-out effects lead to a tendency for a red-shift from the Mie frequency and a mixing of resonance modes when the size of the cluster decreases. The eigenmodes fulfil the linear energy-weighted sum rule, the inverse energy-weighted sum rule and orthogonality relations.

1. Introduction

In recent years the study of the electronic response of small metal particles to external fields has received much attention; for reviews see [1, 2]. The most complete theory available is the time-dependent local density approximation (TDLDA) [3–6], based on the mean-field density functional theory (DFT), within the local density approximation for treating the electron–electron interaction [7]. This theory has reproduced the gross features of the experimental findings [8–10]. The second author studied some applications of this theory including the polarization of the spin [11]. It is worth emphasizing that the RPA [12] is the small-amplitude limit of the TDLDA and the two methods are equivalent as regards studying the energy spectrum of these systems. However, the TDLDA or a full RPA requires a large numerical effort and the calculations soon become prohibitive when the number of atoms is increased. It is important to discover whether simpler approximations are able to reproduce the main physical results of this theory. Related to the TDLDA and RPA are the sum-rule [13, 14] and nuclear fluid-dynamical approaches [15–17].

The sum-rule approach has proven to be extremely useful in describing giant resonances in atomic nuclei [18]. The sum rules concern the integral of the response function weighted with different powers of the frequency. An estimate of the frequency of the plasmon may be obtained from two sum rules assuming that one state exhausts the sum rules. The easiest one to evaluate is the well known Thomas–Reiche–Kuhn (TRK) sum rule. Bertsch and Ekardt, in their work [19], concentrated on the cubic energy-weighted sum (m_3), which can be expressed in a closed form, and they derived a formula for the plasmon ($\ell = 1$) in finite spherical

0953-8984/99/438459+18$30.00

metal particles. They showed that the plasmon in a jellium model is red-shifted from the Mie frequency when the size of the cluster decreases.

Serra and co-workers [20] have extended the work of Bertsch and Ekardt to all multipole surface modes and they have also presented some results for the $\ell = 0$ volume mode. In the dipole case ($\ell = 1$), only the jellium–electron Coulomb energy contributes to m_3. The kinetic and electron–electron Coulomb contributions vanish because the operator $rY_{1,0}$ corresponds to a translation of the electron cloud as a whole. Only the translational-symmetry-breaking jellium field gives a non-zero contribution. They have also obtained the well known red-shift of the energies of plasmons due to the diffuseness of the electron density. For the higher multipolarities ($\ell > 1$), the m_3-sum rule will consist of three terms, coming from the kinetic energy density, from the electron–electron Coulomb energy and from the jellium–electron Coulomb energy. Pure volume terms like the Coulomb-exchange contribution and the correlation energy do not contribute to m_3.

Brack [21] has proposed a semiclassical extension of the RPA sum-rule approach for calculating estimates of the peak positions and widths of collective multipole excitations of the electrons. He has arrived at the same expressions for m_3 using a similar technique, but using a trial Thomas–Fermi density instead of the quantal Kohn–Sham density and taking the fourth-order gradient corrections to the kinetic energy. He has used a multidimensional extension of the sum-rule approach to study the coupling of surface and volume plasmons for all multipolarities, introducing a set of trial operators $Q_\ell^p = r^p Y_{\ell,0}$ for each multipolarity, with p being a positive number. He obtained a matrix equation leading to M eigenmodes, for each multipolarity ℓ, with frequencies ω_m. These modes satisfy the orthogonality relations and fulfil the linear and the cubic energy-weighted sum rules.

Reinhard and Brack in their work with Genzken [22] have introduced a representation of the RPA in terms of coordinate-like operators Q and momentum-like operators P. They have derived a variational principle for Q-variation. In particular, they have discussed a restricted set of local operators $Q(r)$ leading to a differential equation quite similar to the nuclear fluid-dynamical equations. The practical solution of the collective eigenvalue problem for a given multipolarity proceeds via a power expansion of $Q(r)$ and the solution of a secular equation for coupled modes.

On the other hand, semiclassical methods have provided a possible alternative for studying the properties of heavy nuclei [23–28] and their use has proved to be particularly fruitful in this area. These methods are rather intuitive and they have a great physical appeal since they describe the collective motion in terms of physically meaningful quantities, such as the current density. These quantities are related to the distribution function f in $\boldsymbol{r}, \boldsymbol{p}$-space. The calculations involved in solving the semiclassical problem have the advantage of being simpler than a full quantum mechanical calculation. The numerical effort involved in these calculations does not depend on the number of atoms of the metal cluster, and therefore they can be applied to arbitrarily large systems. Related models have recently been applied to describe the dynamics of the valence electrons in a metal cluster and of the valence electrons in the metal surrounding a spherical cavity (void) [29, 30]. The hydrodynamic equations are solved by means of a variational principle; the result obtained is a simultaneous description of the surface and volume modes of the valence electrons. In references [29, 30] the equilibrium density of the valence electrons has been considered as a step function with the following shape: $n_0(r) = n_0(0)\theta(R - r)$, where $n_0(0)$ is the bulk equilibrium density of the valence electrons. In references [29, 30] the energy of the surface plasmon ($\ell = 1$) is independent of the size of clusters and is equal to the Mie value, $\hbar\omega = \hbar\omega_p/\sqrt{3}$ where $\hbar\omega_p$ stands for the energy of the bulk volume plasmon.

In this paper we investigate the effect that the profile of the equilibrium density of the

valence electrons has on the collective modes obtained within the hydrodynamic model. We take into account in the energy density a term involving derivatives of the density which is associated with the valence electron density spillage outside of the domain occupied by the jellium. The consideration of the effect of the spill-out of the valence electrons is expected to contribute to a better description of the collective modes of the valence electrons. To our knowledge, this is the first time that a quantal electronic density has been considered within the hydrodynamic model.

The paper is organized as follows. We shall describe how we obtain the electronic density of the equilibrium state in section 2. The Lagrangian and equations of motion will be briefly reviewed in section 3 and the orthogonality and sum rules in section 4. In section 5 the polynomial approximation used in this work will be discussed. The numerical results for the surface and volume modes and the sum rules will be presented in section 6. Finally, we shall make some concluding remarks in section 7.

2. The equilibrium state

In order to study small-amplitude vibrations we start by determining the equilibrium density of the valence electrons in a metal cluster.

In the classical limit the Wigner transform of the single-particle density matrix is a function $f(\boldsymbol{r}, \boldsymbol{p}, t)$ which acts as a distribution function in $\boldsymbol{r}$, $\boldsymbol{p}$-space. To describe the equilibrium state of the gas of valence electrons, we consider a Fermi-type distribution function:

$$f_0 = \Theta\left(\mu_0 - \frac{p^2}{2m} - U_0(r)\right) \tag{1}$$

where μ_0 is the chemical potential and $U_0(r)$ is the self-consistent equilibrium potential. We assume that in the equilibrium state the energy of the system is represented by the following LDA functional $E[n]$ proposed in reference [31]:

$$E[n] = \sum_{p=1}^{3} \tau_p \int \mathrm{d}\boldsymbol{x}\, n^{\gamma_p} + \frac{\hbar^2\lambda}{8m}\int \frac{(\nabla n)^2}{n}\,\mathrm{d}\boldsymbol{x} - e\int V(\boldsymbol{x})n(\boldsymbol{x})\,\mathrm{d}\boldsymbol{x} + \frac{1}{2}\frac{e^2}{4\pi\epsilon_0}\int\int \frac{n(\boldsymbol{x}_1)n(\boldsymbol{x}_2)}{|\boldsymbol{x}_1 - \boldsymbol{x}_2|}\,\mathrm{d}\boldsymbol{x}_1\,\mathrm{d}\boldsymbol{x}_2 \tag{2}$$

where

$$\tau_1 = \frac{3\hbar^2}{10m}(3\pi^2)^{2/3} \qquad \tau_2 = -\frac{3}{4}\left(\frac{3}{\pi}\right)^{1/3}\frac{\hbar^2}{ma_0} \qquad \tau_3 = -0.0635\left(\frac{4\pi}{3}\right)^{1/6}\frac{\hbar^2}{ma_0^{3/2}}. \tag{3}$$

$\gamma_1 = 5/3$, $\gamma_2 = 4/3$, $\gamma_3 = 7/6$; a_0 is the Bohr radius; n stands for the density of valence electrons. The mean field $V(\boldsymbol{x})$, created by the positive ions, is obtained in the spherical-jellium approximation, which has been used to explain many of the properties of metal clusters [32–36]. The Weizsäcker term $(\hbar^2\lambda/8m)[(\nabla n)^2/n]$ appearing in the energy density has a big influence on the electron surface diffuseness and on the exponential fall-off of the electron density as well.

The equilibrium density is obtained by minimizing the energy functional with respect to n, using the constraint that the total number of valence electrons is fixed. We have

$$\delta(E - \mu_0 N) = 0 \tag{4}$$

where N stands for the total number of valence electrons. The self-consistent equilibrium density n_0 fulfils the equation

$$\frac{\delta E}{\delta n} = \mu_0. \tag{5}$$

3. The Lagrangian and equations of motion

The time-dependent distribution function f describing some type of motion of the system is related to the equilibrium distribution function f_0 by means of a time-dependent canonical transformation:

$$f = f_0 + \{f_0, S\} + \frac{1}{2}\{\{f_0, S\}, S\} + \cdots \tag{6}$$

where the curly brackets $\{\ ,\ \}$ stand for the Poisson brackets. The time-dependent generator S determines the type of motion that the system is exhibiting. Such a generator appears as a solution of the Vlasov equation. Since we consider small-amplitude vibrations, we will be concerned with the linearized Vlasov equation. The generator S may be decomposed into a time-even part Q and a time-odd part P:

$$S(\boldsymbol{x}, \boldsymbol{p}, t) = Q(\boldsymbol{x}, \boldsymbol{p}, t) + P(\boldsymbol{x}, \boldsymbol{p}, t). \tag{7}$$

We consider a restricted variational space for the generator S and we obtain approximate solutions by means of the quantum mechanical variational principle. An explicit expression for the generator Q may be obtained by considering a general expansion in powers of the momentum (including only even powers of the momentum) and truncating the expansion at some point. In this paper we only consider the lowest-order truncation scheme:

$$Q = \psi(\boldsymbol{x}, t). \tag{8}$$

For the generator P, instead of considering an analogous expansion in powers of the momentum, we define P as the generator of a canonical transformation such that the following equation is satisfied:

$$f_0 + \{f_0, P\} + \frac{1}{2}\{\{f_0, P\}, P\} + \cdots = \Theta\left(\mu_0 - \frac{p^2}{2m} - U_0(r) - W(\boldsymbol{x}, t)\right). \tag{9}$$

We consider the quantum mechanical Lagrangian

$$L = \mathrm{i}\overline{h}\langle\phi|\dot{\phi}\rangle - \langle\phi|H|\phi\rangle \tag{10}$$

and a time-dependent Slater determinant $|\phi\rangle$, which is related to the Slater determinant $|\phi_0\rangle$ describing the ground state by means of the unitary transformation

$$|\phi\rangle = \exp(\mathrm{i}\hat{S}/\overline{h})|\phi_0\rangle \tag{11}$$

where $\hat{S} = \hat{Q} + \hat{P}$ is a one-body time-dependent Hermitian generator. The generators Q and P defined in equations (8) and (9) are the classical limit of the Wigner transforms of the Hermitian time-dependent operators $\hat{Q}$ and $\hat{P}$. Here, and in the following equations, the dots over the dynamical fields indicate time derivatives. For small-amplitude deviations from the equilibrium state, one obtains, up to second order in $\hat{S}$, the following harmonic Lagrangian:

$$L^{(2)} = \frac{\mathrm{i}}{2\overline{h}}\langle\phi_0|[\hat{S}, \dot{\hat{S}}]|\phi_0\rangle - \frac{1}{2\overline{h}^2}\langle\phi_0|[\hat{S}, [H, \hat{S}]]|\phi_0\rangle. \tag{12}$$

Considering the classical limit of the Wigner transform of the quantal Lagrangian (12) and taking into account the parametrization of S indicated by the equations (8) and (9), we write the following semiclassical effective Lagrangian:

$$L^{(2)} = -\int \mathrm{d}\boldsymbol{x}\, n_1\dot{\psi} - T^{(2)}[\psi] - E^{(2)}[n_1] \tag{13}$$

where

$$T^{(2)}[\psi] = \frac{1}{2m}\int \mathrm{d}\boldsymbol{x}\; n_0(\boldsymbol{\nabla}\psi)\cdot(\boldsymbol{\nabla}\psi) \tag{14}$$

$$E^{(2)}[n_1] = \frac{1}{2}\frac{e^2}{4\pi\epsilon_0}\int\int \mathrm{d}\boldsymbol{x}_1\,\mathrm{d}\boldsymbol{x}_2\;\frac{n_1(\boldsymbol{x}_1)n_1(\boldsymbol{x}_2)}{|\boldsymbol{x}_1-\boldsymbol{x}_2|} + \sum_{p=1}^{3}\frac{1}{2}\tau_p\gamma_p(\gamma_p-1)\int \mathrm{d}\boldsymbol{x}\; n_0^{\gamma_p-2}n_1^2$$
$$+\frac{\overline{h}^2\lambda}{8m}\int \mathrm{d}\boldsymbol{x}\;\frac{1}{n_0}\left[(\boldsymbol{\nabla}n_1)\cdot(\boldsymbol{\nabla}n_1) - 2(\boldsymbol{\nabla}n_0)\cdot(\boldsymbol{\nabla}n_1)\frac{n_1}{n_0}\right] \tag{15}$$

and $n_1 = n - n_0$ is the fluctuation of the density.

The action integral should be stationary if we allow for arbitrary variations of the collective coordinates ψ and n_1:

$$\delta\int_{t_1}^{t_2}\mathrm{d}t\;(L+\mu N)^{(2)} = 0 \tag{16}$$

where the Lagrange multiplier μ takes care of the particle number conservation:

$$\int \mathrm{d}\boldsymbol{x}\; n_1 = 0.$$

Since the variations $\delta\psi$ and δn_1 are arbitrary, the equations of motion of the system follow:

$$\dot{n}_1 + \boldsymbol{\nabla}\cdot\left(\frac{n_0}{m}\,\boldsymbol{\nabla}\psi\right) = 0 \tag{17}$$

$$\dot{\psi} + \frac{\delta E^{(2)}[n_1]}{\delta n_1} - \mu_1 = 0 \tag{18}$$

where

$$\frac{\delta E^{(2)}[n_1]}{\delta n_1} = \frac{e^2}{4\pi\epsilon_0}\int \mathrm{d}\boldsymbol{x}_2\;\frac{n_1(2)}{|\boldsymbol{x}_1-\boldsymbol{x}_2|} + \sum_{p=1}^{3}\tau_p\gamma_p(\gamma_p-1)n_0^{\gamma_p-2}n_1$$
$$+\frac{\overline{h}^2\lambda}{4m}\left[-\boldsymbol{\nabla}\cdot\left(\frac{\boldsymbol{\nabla}n_1}{n_0}\right) + \boldsymbol{\nabla}\cdot\left(\frac{n_1}{n_0^2}\,\boldsymbol{\nabla}n_0\right) - \frac{1}{n_0^2}(\boldsymbol{\nabla}n_0)\cdot(\boldsymbol{\nabla}n_1)\right] \tag{19}$$

and $\mu_1 = \mu - \mu_0$. We note that the Lagrangian multiplier μ only applies to $\ell = 0$. For $\ell > 0$ it follows automatically from the orthogonality of the spherical harmonics that

$$\int \mathrm{d}\boldsymbol{x}\; n_1 = 0.$$

4. Orthogonality and sum rules

The variational principle has the advantage that it is related to important sum rules which are fulfilled by the solutions of the equations of motion. This allows us to study the strength associated with the different eigenmodes. We seek solutions of the form

$$A(\boldsymbol{x},t) = \sum_j \overline{A}^{(j)}(\boldsymbol{x})\sin(\omega_j t + \delta_j) \tag{20}$$

for the field n_1 and of the form

$$B(\boldsymbol{x},t) = \sum_j \overline{B}^{(j)}(\boldsymbol{x})\cos(\omega_j t + \delta_j) \tag{21}$$

for the velocity potential ψ.

Using equation (17) and replacing $\delta\psi$ by $\psi^{(i)}$, it is easy to show that

$$\int \mathrm{d}\boldsymbol{x}\ \frac{n_0}{2m}(\boldsymbol{\nabla}\psi^{(i)})\cdot(\boldsymbol{\nabla}\psi^{(j)}) = \frac{1}{2}\int \mathrm{d}\boldsymbol{x}\ \psi^{(i)}\dot{n}_1^{(j)} = \frac{1}{2}\int \mathrm{d}\boldsymbol{x}\ \psi^{(j)}\dot{n}_1^{(i)}. \tag{22}$$

Using equations (18) and (19) it may be seen that

$$\begin{aligned}\frac{1}{2}\frac{e^2}{4\pi\epsilon_0}\int\int \mathrm{d}\boldsymbol{x}_1\,\mathrm{d}\boldsymbol{x}_2\ \frac{\dot{n}_1^{(i)}(1)\dot{n}_1^{(j)}(2)}{|\boldsymbol{x}_1-\boldsymbol{x}_2|} + \sum_{p=1}^{3}\frac{1}{2}\tau_p\gamma_p(\gamma_p-1)\int \mathrm{d}\boldsymbol{x}\ n_0^{\gamma_p-2}\dot{n}_1^{(i)}\dot{n}_1^{(j)}\\ + \frac{\overline{h}^2\lambda}{8m}\int \mathrm{d}\boldsymbol{x}\ \frac{1}{n_0}\Bigg[(\boldsymbol{\nabla}\dot{n}_1^{(i)})\cdot(\boldsymbol{\nabla}\dot{n}_1^{(j)}) - (\boldsymbol{\nabla}n_0)\cdot(\boldsymbol{\nabla}\dot{n}_1^{(i)})\frac{\dot{n}_1^{(j)}}{n_0}\\ - (\boldsymbol{\nabla}n_0)\cdot(\boldsymbol{\nabla}\dot{n}_1^{(j)})\frac{\dot{n}_1^{(i)}}{n_0}\Bigg]\\ = \frac{1}{2}\int \mathrm{d}\boldsymbol{x}\ \dot{n}_1^{(i)}\frac{\delta E^{(2)}[\dot{n}_1^{(j)}]}{\delta\dot{n}_1^{(j)}} = -\frac{1}{2}\int \mathrm{d}\boldsymbol{x}\ \dot{n}_1^{(i)}\ddot{\psi}^{(j)} = \frac{1}{2}\omega_j^2\int \mathrm{d}\boldsymbol{x}\ \dot{n}_1^{(i)}\psi^{(j)}.\end{aligned} \tag{23}$$

From equations (22) and (23) we obtain the orthogonality relations. We write

$$n_1^{(j)}(\boldsymbol{x},t) = \overline{n}_1^{(j)}(\boldsymbol{x})\alpha_j(t)$$
$$\psi^{(j)}(\boldsymbol{x},t) = \overline{\psi}^{(j)}(\boldsymbol{x})\beta_j(t)$$

where $\alpha_j \propto \sin(\omega_j t+\delta_j)$ and $\beta_j \propto \cos(\omega_j t+\delta_j)$. It may be easily seen that if $\omega_i^2 \neq \omega_j^2$, then the orthogonality relations may be written as follows:

$$\frac{1}{2}\int \mathrm{d}\boldsymbol{x}\ \overline{n}_1^{(i)}\overline{\psi}^{(j)} = \delta_{ij}. \tag{24}$$

This model satisfies the energy-weighted sum rule (for m_1) as well as the inverse energy-weighted sum rule (for m_{-1}). Let

$$\hat{D} = \sum_{i=1}^{N} D(\boldsymbol{x}_i)$$

be an excitation operator. We expand $D(\boldsymbol{x})$ in the basis of the eigenfunctions $\overline{\psi}^{(j)}$:

$$D(\boldsymbol{x}) = \sum_j c_j\overline{\psi}^{(j)}(\boldsymbol{x}) = \sum_j c_j\psi^{(j)}(\boldsymbol{x},0)$$

where in equations (20) and (21) all the δ_j were taken to be zero, since

$$c_j = \frac{1}{2}\int \mathrm{d}\boldsymbol{x}\ D\overline{n}_1^{(j)}. \tag{25}$$

Following references [28, 30], it may be shown that the present model fulfils the m_1-sum rule:

$$\sum_j \omega_j c_j^2 = m_1 \equiv T^{(2)}[D] \tag{26}$$

and the m_{-1}-sum rule:

$$\sum_j \frac{c_j^2}{\omega_j} = m_{-1} \equiv E^{(2)}[n_1]. \tag{27}$$

The field n_1 in equation (27) is such that $n = n_0 + n_1$ is the polarization density associated with the external potential D.

5. Polynomial approximation

Instead of solving exactly the equations of motion (17) and (18), it is more convenient to look for approximate solutions using a variational method. We make an expansion of the dynamical fields ψ and n_1 in multipoles and, for each multipolarity, we express the radial dependence as follows:

$$\psi = \sum_{k=k_{min}}^{k_{max}} a_k(t) r^k Y_{\ell 0} \tag{28}$$

$$n_1 = \left(n_0 \sum_{k=q_{min}}^{q_{max}-1} b_k(t) r^k + b_{q_{max}}(t) \frac{\mathrm{d}n_0}{\mathrm{d}r} \right) Y_{\ell 0} \tag{29}$$

where k assumes all the integer values between k_{min} and k_{max} (or q_{min} and $q_{max} - 1$), $q_{max} = q_{min} + n_{dim} - 1$ and $k_{max} = k_{min} + n_{dim} - 1$. In the expansion for n_1 we have introduced a term proportional to $\mathrm{d}n_0/\mathrm{d}r$ because we expect such a term to be important for describing surface modes. We have associated the same number n_{dim} of variational parameters with both fields ψ and n_1. We choose $k_{min} = q_{min} = 0$. The truncation scheme that we choose for the numerical calculations is determined by the value of n_{dim}. We now consider the effective Lagrangian given by equations (13)–(15) to obtain approximate solutions of the equations (17) and (18).

Inserting expressions (28) and (29) into equations (13)–(15), we write out the Lagrangian

$$L^{(2)} = \sum_{kq} \left[C_{kq} a_k \dot{b}_q - \frac{1}{2m} A_{kq} a_k a_q - \frac{1}{2} B_{kq} b_k b_q \right] \tag{30}$$

where

$$A_{kj} = \int \mathrm{d}r \; n_0 r^{k+j} [kj + \ell(\ell+1)] \tag{31}$$

$$C_{kj} = \int \mathrm{d}r \; r^{2+k} \tilde{n}_1(j, r) \tag{32}$$

$$\begin{aligned} B_{kj} = {} & \frac{e^2}{4\pi\epsilon_0} \frac{4\pi}{2\ell+1} \left\{ \int_0^\infty \mathrm{d}r_1 \; r_1^{-\ell+1} \tilde{n}_1(k, r_1) \int_0^{r_1} \mathrm{d}r_2 \; r_2^{\ell+2} \tilde{n}_1(j, r_2) \right\} \\ & + \frac{e^2}{4\pi\epsilon_0} \frac{4\pi}{2\ell+1} \left\{ \int_0^\infty \mathrm{d}r_2 \; r_2^{-\ell+1} \tilde{n}_1(j, r_2) \int_0^{r_2} \mathrm{d}r_1 \; r_1^{\ell+2} \tilde{n}_1(k, r_1) \right\} \\ & + \frac{\lambda\hbar^2}{4m} \int \mathrm{d}r \; r^2 \frac{1}{n_0} \left\{ \frac{\mathrm{d}\tilde{n}_1(k, r)}{\mathrm{d}r} \frac{\mathrm{d}\tilde{n}_1(j, r)}{\mathrm{d}r} + \frac{\ell(\ell+1)}{r^2} \tilde{n}_1(k, r) \tilde{n}_1(j, r) \right\} \\ & - \frac{\lambda\hbar^2}{4m} \int \mathrm{d}r \; r^2 \frac{1}{n_0^2} \frac{\mathrm{d}n_0}{\mathrm{d}r} \left\{ \frac{\mathrm{d}\tilde{n}_1(k, r)}{\mathrm{d}r} \tilde{n}_1(j, r) + \frac{\mathrm{d}\tilde{n}_1(j, r)}{\mathrm{d}r} \tilde{n}_1(k, r) \right\} \\ & + \sum_{p=1}^{3} \tau_p \gamma_p (\gamma_p - 1) \int \mathrm{d}r \; r^2 n_0^{\gamma_p - 2} \tilde{n}_1(k, r) \tilde{n}_1(j, r). \end{aligned} \tag{33}$$

We have defined

$$n_1 = \sum_k b_k(t) \tilde{n}_1(k, r) Y_{\ell 0}$$

where

$$\tilde{n}_1(k, r) = \begin{cases} r^k n_0 & \text{if } q_{min} \leqslant k < q_{max} \\ \dfrac{\mathrm{d}n_0}{\mathrm{d}r} & \text{if } k = q_{max}. \end{cases}$$

On requiring the action integral to be stationary for arbitrary variations of the variables a_q and b_q, the following equations are obtained:

$$\sum_q \left(C_{kq}\dot{b}_q - \frac{1}{m} A_{kq} a_q \right) = 0 \tag{34}$$

and

$$\sum_k (-C_{kq}\dot{a}_k - B_{kq} b_q) = 0. \tag{35}$$

We assume harmonic time dependence for the variables a_k and b_k. The eigenmodes are then easily obtained from equations (34) and (35):

$$m\omega^2[b] = [C^{\mathrm{T}}]^{-1}[A][C]^{-1}[B][b] \tag{36}$$

where: $[a]$ and $[b]$ are the vectors with components a_k and b_k; and $[A]$, $[B]$ and $[C]$ are the matrices with components A_{ik}, B_{ik} and C_{ik}. Solving the eigenvalue equation we obtain the normal modes, which are characterized by the eigenfrequencies ω_j and the eigenvectors $[a]^{(j)}$. The vectors $[b]^{(j)}$ are easily obtained.

We have developed a computer program for solving this equation, which is a numerical equation. In previous works which have used the hydrodynamic approach, the electronic equilibrium density was a step function and the calculations were easier. Now we work with quantal electronic densities and the difficulty increases.

6. Numerical results

We study the collective modes of sodium clusters with atomic numbers, N, from 8 to 1000. First of all, we need the equilibrium density of the valence electrons. The densities in figure 1 correspond to the Na_{92} cluster. The chain curve is the density obtained from the equilibrium equation (5) using $\lambda = 0.05$. The full and dashed curves are the densities obtained from the analytical expression given in [31] for $\lambda = 0.05$ and $\lambda = 0.2$, respectively. Also shown is the jellium constant density. We can see from this figure that the spill-out of the density increases when λ increases. The results presented in this article correspond to $\lambda = 0.05$.

The self-consistent equilibrium density is obtained from equation (5), using an appropriate computational program. However, this is a process with a slow convergence, especially for large clusters. Thus, in this work we have used the analytical expression for the density proposed in [31], which is much easier to handle.

One of the main advantages of the hydrodynamic approach is the fact that for each choice of n_{dim} we obtain, for each multipolarity ℓ, n_{dim} excited states of the system and not only the 'most collective' state, as in the sum-rule-based formalisms [19, 20]. In this way we can study very easily the coupling between the surface and volume plasmons for all multipolarities as pointed out by Ekardt [6] in the dipole case. The eigenvalue equation (35) may be compared with equation (30) of reference [21], which was derived from a multidimensional extension of the sum-rule approach and also to equation (58) of reference [22] derived from the random-phase approximation (RPA) in the Q–P representation.

Our method yields the best possible results, within the approximation fixed by equations (8) and (9), if we fix k_{min} and q_{min} at the minimum allowed values ($k_{min} = q_{min} = 0$) and allow simultaneously $n_{dim} \to \infty$. Including all terms of an expansion of the generator S would lead to the formulation of an exact classical RPA. As an example, in table 1 we give the energies of the eigenmodes appearing for $\ell = 1$ for different values of n_{dim} ($k_{min} = q_{min} = 0$). Each time that we increase n_{dim} by one unit we are adding a new term in expansions (28) and (29), and as a consequence a new normal mode appears which has the particularity of

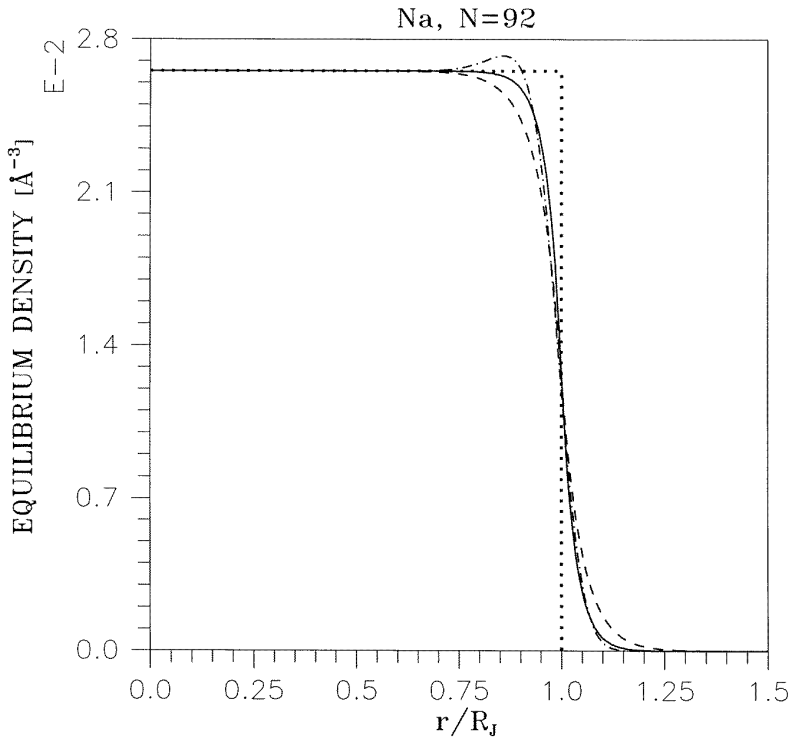

Figure 1. The self-consistent equilibrium density (chain curve) of a cluster of sodium with $N = 92$ atoms and $\lambda = 0.05$, obtained from equation (5), is plotted as a function of r/R_J, where r is the radial distance from the centre and R_J is the radius of the jellium. For comparison the analytical density ($N = 92$, $\lambda = 0.05$) derived in reference [31] is given, as the continuous curve. Increasing the value of λ leads to a larger spill-out as may be seen by considering the dashed curve which represents the analytical density ($N = 92$, $\lambda = 0.2$).

Table 1. For the multipolarity $\ell = 1$, we give the energies of the eigenmodes for different truncation schemes (corresponding to $2 \leqslant n_{dim} \leqslant 6$) in order to study the convergence of the present model. We have considered a sodium cluster having 1000 atoms.

$\hbar\omega_i$	$n_{dim} = 2$	$n_{dim} = 3$	$n_{dim} = 4$	$n_{dim} = 5$	$n_{dim} = 6$
$\hbar\omega_1$	3.32	3.39	3.39	3.38	3.38
$\hbar\omega_2$	7.76	5.86	5.72	5.69	5.67
$\hbar\omega_3$		8.94	6.09	6.09	6.08
$\hbar\omega_4$			10.1	6.24	6.16
$\hbar\omega_5$				11.4	6.76
$\hbar\omega_6$					13.5

being the eigenmode with the highest energy. When increasing n_{dim}, the energies of the lower eigenmodes for big clusters show up as being very stable with respect to the values that they possessed in the previous truncation scheme. We can conclude from table 1, referring to Na_{1000}, that the convergence is faster for the lower modes, which are, therefore, especially stable. On the other hand, the convergence becomes worse as the size of cluster decreases

even for the lower modes. When we study a cluster with a quantal electron density, perfect numerical stability in our calculation is more difficult to obtain. Reinhard and co-workers in their work [22] discussed the convergence of the expansion method, with respect to the number M of coupled modes (equivalent to our n_{dim}) and to the powers p_α of the operators used to obtain the eigenmode spectrum. They found that for values of the powers ($\delta p_\alpha \leqslant 1$) that are too close, the convergence becomes worse. This might be the reason for the inferior convergence for small clusters in our work.

An interesting aspect is the N-dependence of the energies of the eigenmodes. We give in figures 2–4 the energies of the eigenmodes ($0 \leqslant \ell \leqslant 2$) as obtained in the truncation schemes corresponding to $n_{dim} = 3$, 4 and 5. Firstly, on the basis of these figures we consider the results obtained in the classical limit of a very large cluster; we obtain the following:

- For $\ell = 0$ there is a mode with energy zero (which has no strength) and k_{dim-1} degenerate eigenvalues with the bulk plasma frequency ($\omega = \omega_p$). There exists thus for classical metal spheres only one monopole mode with the bulk plasmon frequency.
- For a fixed multipolarity $\ell > 0$ there are $k_{dim} - 1$ degenerate eigenvalues $\omega = \omega_p$ and one non-degenerate eigenvalue

$$\omega = \omega_\ell = \omega_p(\ell/(2\ell + 1))^{1/2}$$

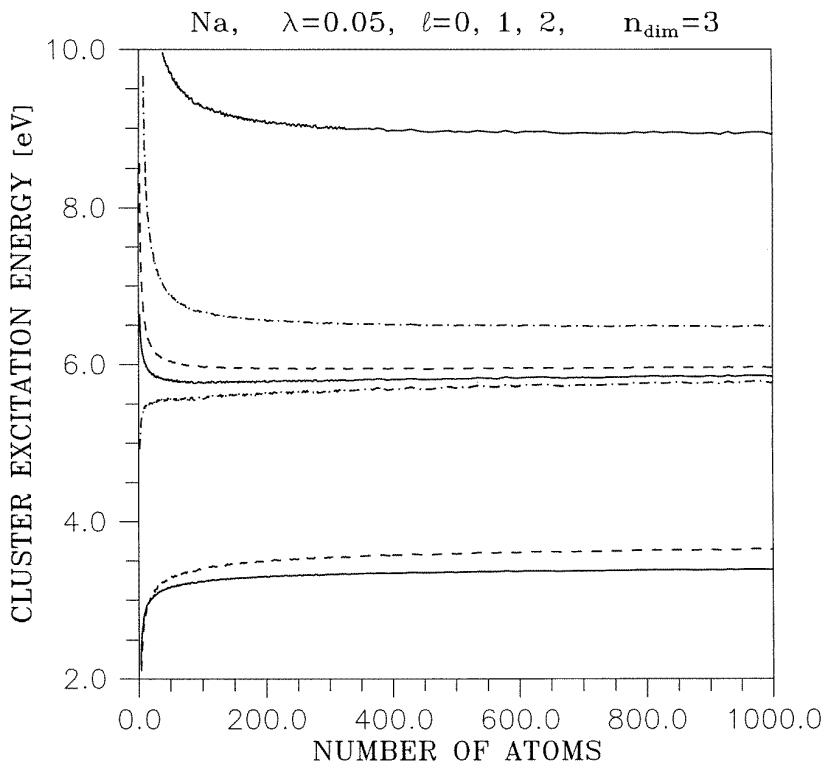

Figure 2. The cluster excitation energy versus the number of atoms of the cluster, for sodium, for angular momenta $0 \leqslant \ell \leqslant 2$. The chain curves refer to $\ell = 0$ normal modes, the full curves refer to $\ell = 1$ normal modes and the dashed curves refer to $\ell = 2$ normal modes. The truncation scheme corresponding to $n_{dim} = 3$ was considered. The equilibrium analytical density proposed in reference [31] was used.

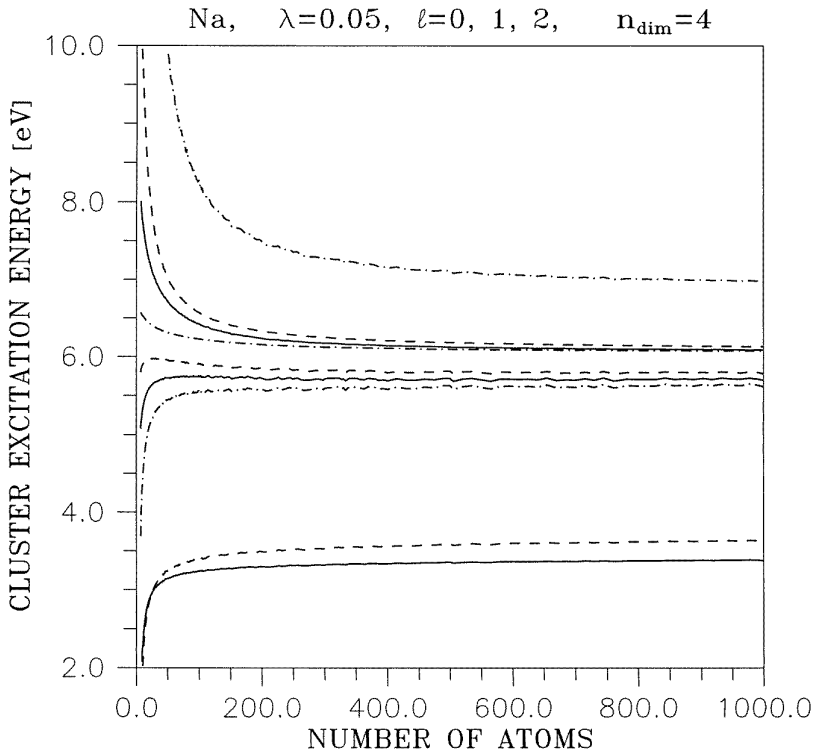

Figure 3. The same results as in figure 2, but for $n_{dim} = 4$.

which is the classical Mie frequency of the surface plasmon. Thus in classical spheres there exists for each multipolarity ℓ a surface plasmon with the Mie frequency and a volume plasmon with the bulk plasmon frequency.

In this way we have found that the classical Mie frequency can be recovered from the hydrodynamic approach by solving the equation (36) for any multipolarity $\ell > 0$. The fact that all volume plasmons are degenerate in this limit means that the eigenvalues of these solutions do not depend on the radial form of the operator Q. This is not surprising since this limit is defined as the one for which the electron density is constant over the whole volume of the cluster.

Secondly, from these figures we can see that in finite clusters the results change due to quantum and size effects. Surface and kinetic energy corrections will shift the energy away from its classical limit for finite clusters. The kinetic energy of the electrons, exchange and correlation effects and the finite spill-out of the density give a finite multipole strength to the volume plasmons. This leads to a fragmentation (Landau damping).

The lower volume plasmon with multipolarity $\ell = 0$ included in these figures is similar to the 'breathing-mode' vibration (giant monopole resonance) of nuclei. The field $Q = r^2$ will generate monopole volume oscillations. The energy of this mode increases when N increases. This behaviour, displayed also in figures 4–6 of reference [20] and figure 3 of reference [21], was not found in previous works [29, 30] of the first author, where the spill-out of the valence electrons outside the jellium was not taken into account. We can say that the diffuseness of the equilibrium density has an important effect on this mode.

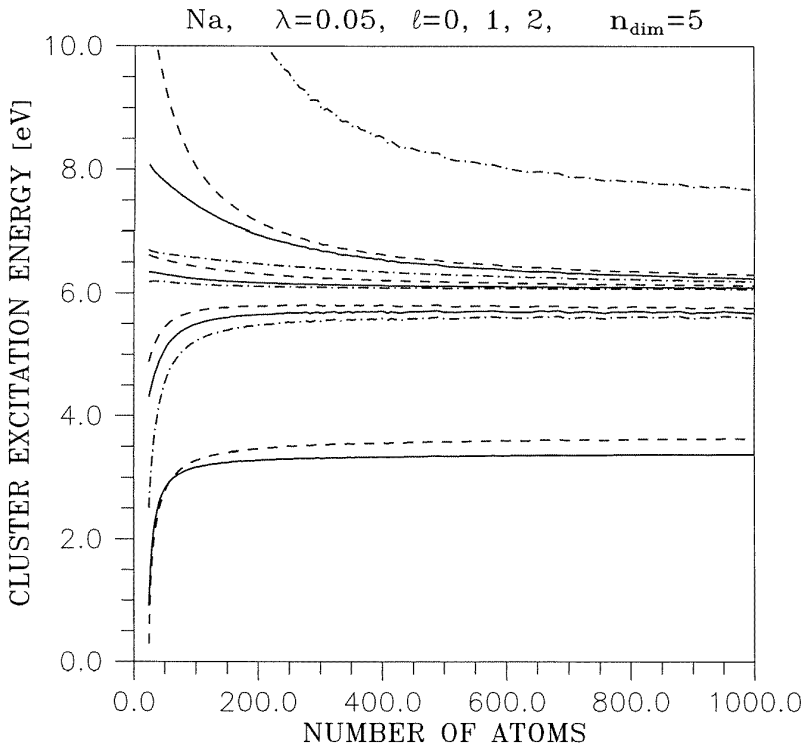

Figure 4. The same results as in figure 2, but for $n_{dim} = 5$.

For $\ell > 0$, the lowest mode corresponds to a pure surface oscillation during which the electron density is translated ($\ell = 1$) or deformed ($\ell > 1$) but not compressed. We want to point out that we obtain the well known red-shift of the dipole plasmon when the size of the cluster decreases. This effect has often been reproduced by sum-rule methods and of course by using the TDLDA but not using the hydrodynamic model. This effect is related to the diffuseness of the electron density, which has not been considered in previous hydrodynamic works [30]. To confirm the possibility, we have calculated for several values of λ the energies of the dipole mode. Figure 5 shows these results. The upper curve corresponds to $\lambda = 0.05$, the middle curve to $\lambda = 0.2$ and the lower curve to $\lambda = 0.5$. We see from this figure that the downwards bending increases when λ increases. Besides the bending, increasing the value of λ also causes a global downwards shift of the curve. Thus, we can conclude that the red-shifting of the dipole mode from the classical Mie value is a surface diffuseness effect in our model.

For the rest of multipolarities ($\ell > 1$) we also found indications of a red-shift of the energies with respect to the Mie value.

The present model satisfies the m_1- and m_{-1}-sum rules. While the m_1-sum has a closed expression which is independent of the truncation scheme n_{dim}-value, the m_{-1}-sum is evaluated by assuming an external potential $D(\boldsymbol{x})$ and by minimizing the energy, for the truncation scheme n_{dim}-value that we are using (in an analogous way to that in reference [30]). We consider the excitation operators $D(\boldsymbol{x}) = r^2$ for $\ell = 0$ and $D(\boldsymbol{x}) = r^\ell Y_{\ell 0}$ for $\ell > 0$.

In tables 2–5 we present the energies of the eigenmodes up to $\ell = 2$ for $N = 1000$ together with the percentages of the m_1- and m_{-1}-sum rules exhausted by each state, considering

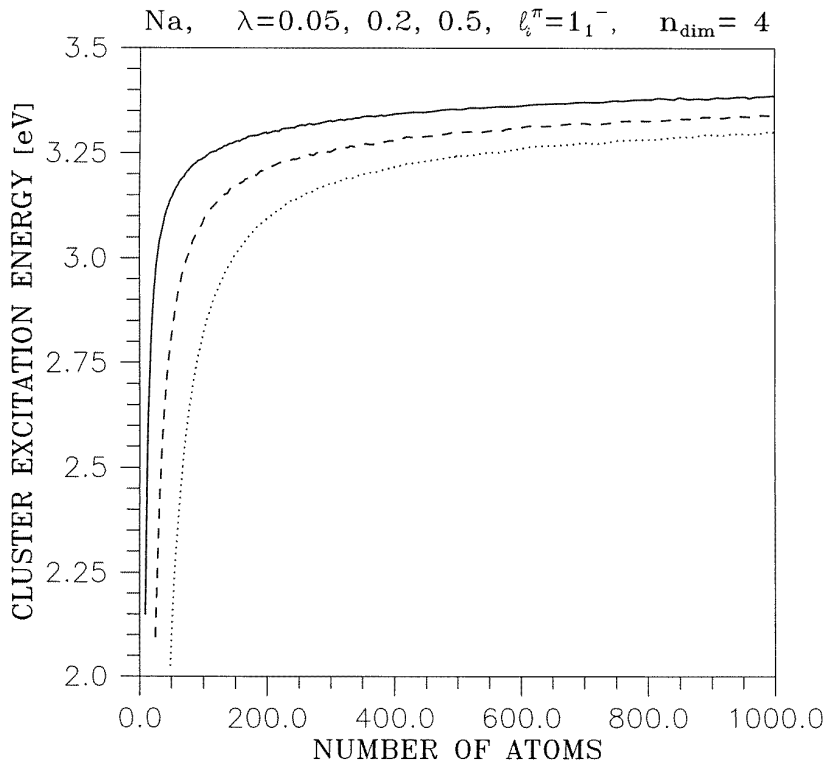

Figure 5. Cluster excitation energies for the lower dipole mode versus the number of atoms of the cluster, for sodium, for different values of λ. The curves correspond to $\lambda = 0.05$ (continuous curve), $\lambda = 0.2$ (dashed curve) and $\lambda = 0.5$ (dotted curve). The truncation scheme corresponding to $n_{dim} = 4$ was considered.

Table 2. For the multipolarities $\ell = 0, 1, 2$, we list the excitation energies (second column), the exhausted percentage of the m_1-sum rule (third column) and the exhausted percentage of the m_{-1}-sum rule (fourth column), for a sodium cluster of $N = 1000$ atoms. The truncation scheme corresponding to $n_{dim} = 3$ was considered. The equilibrium analytical density proposed in reference [31] was used.

ℓ_i^π ($N = 10^3$)	$\hbar\omega_i$ (eV)	m_1 (fraction)	m_{-1} (fraction)
$\ell = 0_1^+$	5.78	9.07×10^{-1}	9.24×10^{-1}
$\ell = 0_2^+$	6.48	9.34×10^{-2}	7.56×10^{-2}
$\ell = 1_1^-$	3.39	9.96×10^{-1}	9.99×10^{-1}
$\ell = 1_2^-$	5.86	3.08×10^{-3}	1.04×10^{-3}
$\ell = 1_3^-$	8.94	5.22×10^{-4}	7.54×10^{-5}
$\ell = 2_1^+$	3.65	9.95×10^{-1}	9.98×10^{-1}
$\ell = 2_2^+$	5.96	3.82×10^{-3}	1.44×10^{-3}
$\ell = 2_3^+$	11.4	7.73×10^{-4}	7.90×10^{-5}

different truncation schemes (corresponding to $n_{dim} = 3, 4, 5, 6$). For each multipolarity $\ell > 0$, the lowest state (surface mode) exhausts almost the complete m_1- and m_{-1}-sum rules

Table 3. The same results as in table 2, but evaluated with $n_{dim} = 4$.

ℓ_i^π ($N = 10^3$)	$\hbar\omega_i$ (eV)	m_1 (fraction)	m_{-1} (fraction)
$\ell = 0_1^+$	5.64	5.79×10^{-1}	6.17×10^{-1}
$\ell = 0_2^+$	6.08	4.05×10^{-1}	3.71×10^{-1}
$\ell = 0_3^+$	6.98	1.61×10^{-2}	1.12×10^{-2}
$\ell = 1_1^-$	3.39	9.94×10^{-1}	9.98×10^{-1}
$\ell = 1_2^-$	5.72	6.15×10^{-3}	2.16×10^{-3}
$\ell = 1_3^-$	6.09	3.93×10^{-5}	1.22×10^{-5}
$\ell = 1_4^-$	10.1	2.21×10^{-4}	2.52×10^{-5}
$\ell = 2_1^+$	3.64	9.89×10^{-1}	9.96×10^{-1}
$\ell = 2_2^+$	5.80	1.05×10^{-2}	4.17×10^{-3}
$\ell = 2_3^+$	6.14	1.34×10^{-4}	4.73×10^{-5}
$\ell = 2_4^+$	13.3	2.79×10^{-4}	2.09×10^{-5}

Table 4. The same results as in table 2, but evaluated with $n_{dim} = 5$.

ℓ_i^π ($N = 10^3$)	$\hbar\omega_i$ (eV)	m_1 (fraction)	m_{-1} (fraction)
$\ell = 0_1^+$	5.61	5.53×10^{-1}	5.94×10^{-1}
$\ell = 0_2^+$	6.07	3.00×10^{-1}	2.76×10^{-1}
$\ell = 0_3^+$	6.19	1.45×10^{-1}	1.28×10^{-1}
$\ell = 0_4^+$	7.69	2.06×10^{-3}	1.18×10^{-3}
$\ell = 1_1^-$	3.38	9.92×10^{-1}	9.97×10^{-1}
$\ell = 1_2^-$	5.69	7.23×10^{-3}	2.57×10^{-3}
$\ell = 1_3^-$	6.09	1.90×10^{-5}	5.90×10^{-6}
$\ell = 1_4^-$	6.24	2.89×10^{-4}	8.54×10^{-5}
$\ell = 1_5^-$	11.4	3.90×10^{-5}	3.45×10^{-6}
$\ell = 2_1^+$	3.63	9.86×10^{-1}	9.94×10^{-1}
$\ell = 2_2^+$	5.77	1.33×10^{-2}	5.31×10^{-3}
$\ell = 2_3^+$	6.13	1.82×10^{-4}	6.46×10^{-5}
$\ell = 2_4^+$	6.30	4.70×10^{-4}	1.58×10^{-4}
$\ell = 2_5^+$	15.6	3.41×10^{-5}	1.87×10^{-6}

and has an energy close to the corresponding Mie value:

$$\hbar\omega_\ell^{(\mathrm{Mie})} = \hbar\omega_p\sqrt{\ell/(2\ell+1)}$$

as has already been discussed. Here $\hbar\omega_p = 6.0495$ eV is the energy of the bulk volume plasmon. Furthermore, in table 6 we give $\hbar\sqrt{\{(m_1/m_{-1})\}}$ which indicates the position of an eigenmode that exhausts fully both the m_1- and m_{-1}-sum rules.

In figure 6 we plot the fractions of the sums m_1 and m_{-1}, respectively, exhausted by the different modes in the truncation scheme corresponding to $n_{dim} = 5$. It is clear that for large values of N and for $\ell > 0$ most of the strength is concentrated in the low-energy mode (surface mode). For small values of N there is a redistribution of the strength. This behaviour was

Table 5. The same results as in table 2, but evaluated with $n_{dim} = 6$.

ℓ_i^π ($N = 10^3$)	$\hbar\omega_i$ (eV)	m_1 (fraction)	m_{-1} (fraction)
$\ell = 0_1^+$	5.58	5.13×10^{-1}	5.57×10^{-1}
$\ell = 0_2^+$	6.07	3.59×10^{-1}	3.30×10^{-1}
$\ell = 0_3^+$	6.11	9.45×10^{-2}	8.57×10^{-2}
$\ell = 0_4^+$	6.51	3.40×10^{-2}	2.72×10^{-2}
$\ell = 0_5^+$	9.11	9.57×10^{-5}	3.91×10^{-5}
$\ell = 1_1^-$	3.38	9.92×10^{-1}	9.97×10^{-1}
$\ell = 1_2^-$	5.67	7.62×10^{-3}	2.73×10^{-3}
$\ell = 1_3^-$	6.08	1.27×10^{-5}	3.95×10^{-6}
$\ell = 1_4^-$	6.16	3.60×10^{-5}	1.09×10^{-5}
$\ell = 1_5^-$	6.76	4.35×10^{-4}	1.09×10^{-4}
$\ell = 1_6^-$	13.5	7.48×10^{-6}	4.74×10^{-7}
$\ell = 2_1^+$	3.63	9.85×10^{-1}	9.94×10^{-1}
$\ell = 2_2^+$	5.75	1.39×10^{-2}	5.60×10^{-3}
$\ell = 2_3^+$	6.10	4.63×10^{-5}	1.66×10^{-5}
$\ell = 2_4^+$	6.29	2.87×10^{-4}	9.64×10^{-5}
$\ell = 2_5^+$	6.82	7.18×10^{-4}	2.05×10^{-4}
$\ell = 2_6^+$	18.9	1.96×10^{-5}	7.26×10^{-7}

Table 6. For the multipolarities listed in the first column, the quantities $\hbar\sqrt{(m_1/m_{-1})}$ are calculated with different values of n_{dim}, where m_1 and m_{-1} are the energy-weighted and the inverse energy-weighted sums. The equilibrium analytical density of [31] for a sodium cluster with $N = 1000$ was used.

ℓ^π ($N = 10^3$)	$\hbar\sqrt{m_1/m_{-1}}$ (eV) ($n_{dim} = 3$)	$\hbar\sqrt{m_1/m_{-1}}$ (eV) ($n_{dim} = 4$)	$\hbar\sqrt{m_1/m_{-1}}$ (eV) ($n_{dim} = 5$)	$\hbar\sqrt{m_1/m_{-1}}$ (eV) ($n_{dim} = 6$)
0^+	5.83	5.82	5.82	5.82
1^-	3.40	3.39	3.39	3.39
2^+	3.66	3.65	3.65	3.65

not apparent in any previous work on clusters where the hydrodynamic model was used. We also see that, as we consider larger values of ℓ, the fraction of the sum rules exhausted by the surface mode decreases. This might suggest that as ℓ increases the strength becomes more distributed.

We see that the spill-out of the valence electrons has a very important role, leading to a red-shift of the energies and also to a mixture of the modes when the number of atoms in the cluster decreases. To our knowledge, this is the first time that such effects, which have already been studied with other methods, have been obtained within the hydrodynamic model.

7. Conclusions

The fluid-dynamical model presented here is based on the Thomas–Fermi approximation. It is able to describe the main features of cluster excitations, giving a good prediction of the excited

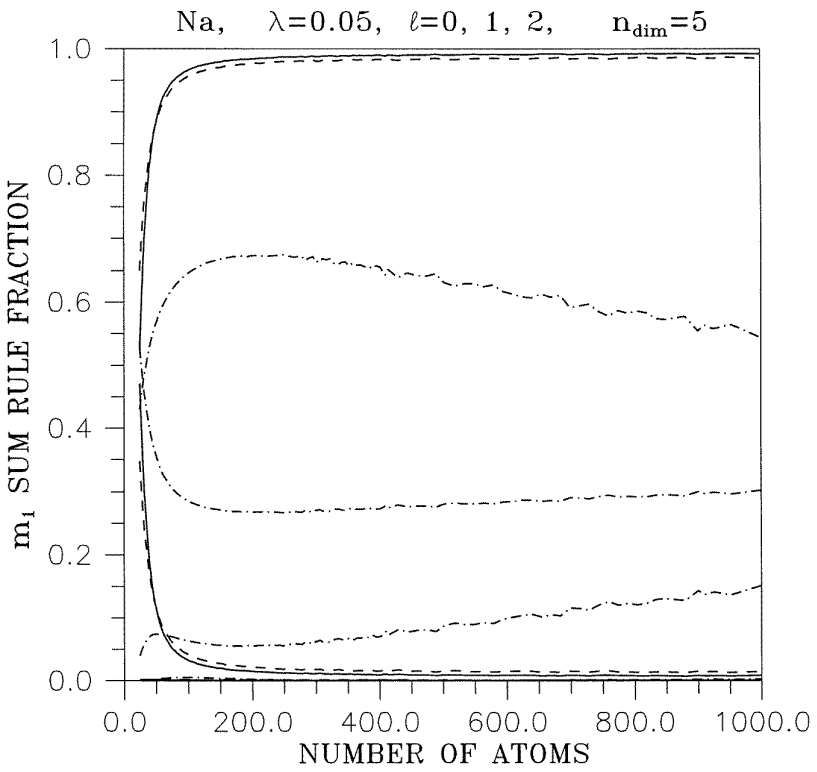

Figure 6. Fractions of the m_1-sum rule versus the number of atoms of the cluster, for sodium, for angular momenta $0 \leqslant \ell \leqslant 2$. The chain curves refer to $\ell = 0$ normal modes, the full curves refer to $\ell = 1$ normal modes and the dashed curves refer to $\ell = 2$ normal modes. The truncation scheme corresponding to $n_{dim} = 5$ was considered.

energies, especially for larger clusters, where microscopic calculations such as TDLDA ones are nearly impossible and semiclassical aspects play a dominant role. It has the advantage of being able to handle clusters with a large number of atoms, not only yielding the excitation energies and the exhausted fractions of important sum rules, but also providing a deeper physical insight.

Sum-rule-based methods are useful tools for investigating collective dynamical properties of many-body systems; however, a fluid-dynamical formulation, such as the one presented here, allows us to access problems which are beyond the scope of a pure sum-rule approach. To our knowledge, all previous works using this hydrodynamic approach have used equilibrium electron densities with a sharp surface (step function) and they are not able to take into account some of the surface effects. In the present article we have followed closely reference [30] where a hydrodynamic description of both volume and surface modes in metal clusters is considered. We have extended the model in order to take into account the spill-out. In order to do this, we have introduced in the energy functional a term with gradients of the density (the Weizsäcker correction) which is connected to a smooth surface profile.

The approximate eigenmodes are obtained by diagonalizing a matrix of dimension $n_{dim} \times n_{dim}$ where n_{dim} is the number of terms introduced in the expansions (28) and (29). For each multipolarity $\ell > 0$, one of these modes is a pure surface oscillation and the other eigenmodes are volume modes which may be interpreted as the remainder of a strongly

fragmented volume plasmon. The $\ell = 0$ modes correspond to spherically symmetrical oscillations of the electron gas. We have recovered the well known classical Mie expression for the energies of the surface modes and we have shown that the energies of the volume modes approach the energy of the volume plasmon.

The normal modes fulfil the energy-weighted sum rule, the inverse energy-weighted sum rule and orthogonality relations.

The main advantage of the present formulation is that we are able to describe the surface modes for large clusters with a small numerical effort—three terms ($n_{dim} = 3$) in the expansions (28) and (29) are already sufficient. For smaller clusters our results seem to indicate the existence of a red-shift and of a redistribution of the strength. These two effects are due to our having taken into account in the equilibrium density the spill-out of the valence electrons.

It should be observed that our approach, being based on the Thomas–Fermi method, is not expected to describe adequately oscillations of particle density with wavelength smaller than the Fermi wavelength. Moreover, it neglects all friction due to electron–electron collisions or of any other origin. As a result, the lifetime of the plasmon mode falls outside the scope of our calculation.

It would be very interesting to compare the spill-out of the electrons, obtained here, with the same spill-out obtained from a full quantal Kohn–Sham calculation. Unfortunately we are not aware of such a calculation.

Acknowledgment

The authors are grateful to L C Balbás for making available programs for evaluating the equilibrium density.

References

[1] De Heer W 1993 *Rev. Mod. Phys.* **65** 611
[2] Brack M 1993 *Rev. Mod. Phys.* **65** 677
[3] Stott M J and Zarembra E 1980 *Phys. Rev.* A **21** 12
[4] Zangwill A and Soven P 1980 *Phys. Rev.* A **21** 1561
[5] Ekardt W 1984 *Phys. Rev. Lett.* **52** 1925
[6] Ekardt W 1985 *Phys. Rev.* B **31** 6360
[7] Jones R O and Gunnarson O 1989 *Rev. Mod. Phys.* **61** 689
[8] Knight W D, Clemenger K, de Heer W A, Saunders W A, Chou M Y and Cohen M L 1984 *Phys. Rev. Lett.* **52** 2141
[9] Knight W D, Clemenger K, de Heer W A and Saunders W A 1985 *Phys. Rev.* B **31** 2539
[10] de Heer W A, Selby K, Kresin V, Masui J, Vollmer M, Chatelain A and Knight W D 1987 *Phys. Rev. Lett.* **59** 1805
[11] Torres M B 1997 *PhD Thesis* Valladolid University
[12] Bohm D and Pines D 1953 *Phys. Rev.* **92** 609
[13] Marshalek E R and da Providência J 1973 *Phys. Rev.* C **7** 2281
[14] Bohigas O, Lane A M and Martorell J 1979 *Phys. Rep.* C **51** 267
[15] Holzwarth G and Eckart G 1978 *Z. Phys.* A **284** 291
[16] da Providencia J P and Holzwarth G 1985 *Nucl. Phys.* A **439** 477
[17] Krivine H, Treiner J and Bohigas O 1980 *Nucl. Phys.* A **366** 155
[18] Lipparini E and Stringari S 1989 *Phys. Rep.* **175** 103
[19] Bertsch G F and Ekardt W 1985 *Phys. Rev.* B **32** 7659
[20] Serra Ll, Garcias F, Barranco M, Navarro J, Balbás C and Mañanes A 1989 *Phys. Rev.* B **39** 8247
[21] Brack M 1989 *Phys. Rev.* B **39** 3533
[22] Reinhard P G, Brack M and Genzken O 1990 *Phys. Rev.* A **41** 5568
[23] da Providencia J P and Holzwarth G 1983 *Nucl. Phys.* A **398** 59
[24] da Providencia J P 1987 *J. Phys. G: Nucl. Phys.* **13** 783

[25] da Providencia J P 1988 *Nucl. Phys.* A **489** 111
[26] da Providencia J, Brito L and Providencia C 1985 *Nuovo Cimento* **87** 248
[27] Brito L and Providencia C 1985 *Phys. Rev.* C **32** 2049
[28] da Providência J Jr 1991 *Nucl. Phys.* A **523** 247
[29] da Providência J Jr and de Haro R Jr 1994 *Phys. Rev.* B **49** 2086
[30] da Providência J Jr 1997 *J. Phys.: Condens. Matter* **9** 2931
[31] Mañanes A, Membrado M, Pacheco A F, Sañudo J and Balbás L C 1994 *Int. J. Quantum Chem.* **52** 767
[32] Martins J, Car R and Buttet J 1981 *Surf. Sci.* **106** 265
[33] Ekardt W 1984 *Phys. Rev.* B **29** 1558
[34] Chou M Y, Cleland A and Cohen M L 1984 *Solid State Commun.* **52** 645
[35] Ekardt W and Penzar Z 1991 *Phys. Rev.* B **43** 1322
[36] Koskinen M, Lipas P O and Manninen M 1995 *Z. Phys.* D **35** 285